



Fabrications and investigation of physicochemical and electrochemical properties of heteropoly acid-doped sulfonated chitosan-based polymer electrolyte membranes for fuel cell applications

J. Kalaiselvimary¹ · M. Ramesh Prabhu¹

Received: 16 February 2018 / Revised: 13 July 2018 / Accepted: 16 July 2018 / Published online: 23 July 2018
© Springer-Verlag GmbH Germany, part of Springer Nature 2018

Abstract

A proton exchange membrane for fuel cell application consists of modified chitosan/PEO doped with different weight percentage of HPA acids cross-linked by sulfosuccinic acid. Modifying the chemical structure of the chitosan by means of sulfonation, which was successfully synthesized by direct sulfonating reagent 1,3-propane sultone, chemical structure and thermal stability of the membrane were characterized by FTIR and TG analysis. Further the membrane was characterized by XRD, SEM, AFM and impedance analysis. The results shows that the structure of the composite membranes becomes more compact compared with undoped membranes due to interaction between the sulfonic acid groups and amine groups. This could lead to increase the conductivity and reduce the excess swelling of the membrane. From all the results, these biodegradable and low-costs composite membrane was tested in the single-cell proton exchange membrane fuel cell and it predicts that chitosan-based electrolytes are promising material for fuel cell application.

Keywords Ion exchange capacity · Physico-chemical characterization · Heteropoly acids · Cross-linked membranes

List of Symbols

σ	Conductivity
σ_0	Pre-exponential factor
E_a	Activation energy
k	Boltzmann constant
t	Thickness of the prepared polymer electrolyte membranes
A	Area of the prepared polymer electrolyte membranes
R_b	Bulk resistance of the electrolyte membranes

✉ M. Ramesh Prabhu
mkram83@gmail.com

¹ Department of Physics, Alagappa University, Karaikudi 630 003, India

μ	Micro
θ	Theta
$^{\circ}\text{C}$	Degree Celsius
\AA	Angstrom
K	Kelvin
$\%T$	Percentage of transmittance

Introduction

Environmental problems and energy security are the biggest challenges for the last 2 decades. The enrollment of anion exchange membrane fuel cells is imperative and stimulated its application as a promising high challenged energy source for zero emission vehicles, high power energy sectors and portable applications [1]. Fuel cell requires a membrane to separate the chemical reactions at the anode from the cathode both chemically and electronically. A successful fuel cell membrane must allow protons to move freely [2]. Alternative to commercial Nafion membranes includes various new modified perfluorinated, partially perfluorinated and non-perfluorinated membranes. In addition to these membranes for last few years, attention has been focused on preparation of organic/inorganic hybrid membranes through sol–gel processes. In the hybrid membranes, thermal stability is provided by the inorganic back bone, while the organic chains confer the required specific properties such as flexibility and process ability [3]. Heteropoly acids are strong Bronsted acid as well as solid electrolytes and are considered promising materials in the fabrication of organic, inorganic nanocomposite membranes for fuel cell application [4]. HPAs are solid crystalline materials, which may adopt the Keggin structure with general formula $\text{H}_3\text{MX}_{12}\text{O}_{40}$ where M is the central atom and X is the heteroatom [5]. Solid heteropoly acid possesses a unique discrete ionic structure including heteropoly anions and counter cations (H^+ , H_3O^+ , H_5O_2^+ , etc.) and consequently exhibits high anion mobility. The HPAs are soluble in polar solvents, where they produce stable acidity of HPAs which is attributed to the large size of the poly anion yielding low delocalized density. The major problems by using HPAs in fuel cell are their solubility is decline in fuel cell performance. To overcome this problem, it has been proposed to prepare chitosan-based HPA-doped electrolyte membranes to be employed as anion exchange membrane in fuel cell, since such polymer electrolyte composites are reported to be insoluble [6]. One promising candidate to act as polymer host for natural ionic polymer is chitosan. A monomer of chitosan consists of hydroxyl and amine functional groups which have lone pair electrons that are suitable for the preparation of solid polymer electrolyte [7]. The existence of lone pair electrons enables the chelating of a proton donor [6, 8]. When a chitosan membrane is swollen in water, the amino groups may be protonated and leaving the hydroxide ions free in water, which may contribute to the ionic conduction in the membrane. Nevertheless, chitosan membranes show low proton conductivity; there is an urgent need to enhance their conductivity. Chitosan also has a high potential for development into sophisticated functional polymers quite different from those of synthetic polymers since it has both free amino and hydroxyl groups on its backbone, which are easily

modified by many organic reactions (tosylation, alkylation, carbocylation, sulfonation, quaternary salt and so on) [9].

The approach adopted in order to improve ionic conductivity in the present work consists of synthesizing composite membranes by incorporation of solid heteropoly acids into sulfonated biopolymer matrices. These super-acidic inorganic oxides are synthetically versatile, exhibit redox catalyst activity and have very high proton conductivity in the solid state. These are known to have strong interactions into which they are doped, resulting in morphological changes as compared with the undoped ionomer [10]. The HPAs, a subset of the polyoxometalates, are an extensive class of structurally well-defined inorganic metal oxide clusters that contain a central heteroatom. These super-acidic inorganic oxides are synthetically versatile, exhibit redox catalyst activity, and have very high proton conductivity in the solid state. These are known to have strong interactions with the sulfonic acid groups of ionomers into which they are doped, resulting in morphological changes, as compared with the undoped polymer membrane.

Organic–inorganic composites as membranes for PEMFC have been investigated with the main objective of increasing the proton conductivity of the membrane. The heteropoly acids are attractive inorganic fillers, because in their crystalline forms these materials have demonstrated to be highly conductive and thermally stable. The presence of phosphotungstic acid and phosphomolybdic acid modifies some important properties of the *s*-chitosan/PEO, such as the increases in the mechanical stability, thermal property as well as their mechanical properties.

Experimental procedures

Materials

Chitosan ($M_w \sim 6 \times 10^5 \text{ g mol}^{-1}$, DA $\sim 85\%$), poly (ethylene oxide) (PEO) of an average molecular weight ~ 8000 , phosphotungstic acid and phosphomolybdic acid, sulfosuccinic acid were purchased from Sigma-Aldrich, German. 1,3-propane sultone and acetic acid were procured from Spectrochem, India.

Sulfonation process of chitosan

The sulfonation of the chitosan may be prepared by the method reported by Tsai et al. [11]. 15 g of chitosan (1% w/w) solution was prepared by adding chitosan powder to 2% (v/v) acetic acid solution, stirring for completely dissolution of chitosan in aqueous acetic acid and then adding 1,3-propane sultone to the solution. The mixture was allowed to react at 60 °C for 10 h. The resulting solution was poured into cold acetone to precipitate. The crude solid was washed sufficiently with methanol to remove the excess 1,3-propane sultone and dried in a vacuum oven at 50 °C over night followed by 120 °C for 6 h. The sulfonated chitosan was obtained as a white powder.

Preparation of polymer nano-composite membrane

Initially, the appropriate amounts of the chosen pair of polymers namely chitosan and PEO corresponding to five different wt% ratios of 90:10, 80:20, 70:30, 60:40 and 50:50, respectively, were dissolved in (10% v/v) aqueous acetic acid solution and the solution mixture was continuously stirred for 6 h at room temperature by means of magnetic stirrer. Subsequently, the solvent was allowed to get evaporated with a constant stirring process performed at room temperature. The homogenous residual solution was cast onto a glass petri dishes followed by a careful vacuum drying procedure carried out at 50 °C over a period of 24 h. Chitosan–PEO blends thus obtained from solution casting technique were found to be 60–80 μm thickness. All such samples were suitably stored in vacuum desiccators for further analysis. In order to obtain a variety of sulfonated chitosan–PEO/HPA-doped electrolyte system, preliminary investigations related to room-temperature impedance spectroscopic measurements were performed on all the freshly prepared sulfonated chitosan–PEO polymer blends. It was found that the optimized composition namely 60:40 wt% ratio of sulfonated chitosan and PEO would possess an appreciably high ionic conductivity at room temperature. Therefore, this particular polymer blend denoted as (s-chitosan:PEO) in all the following sections was treated as the effective host polymer matrix to prepare the different wt% of the heteropoly acids-doped cross-linked electrolyte membranes. Different weight percentage of PWA/PMA were dissolved in respective aqueous acetic acid solutions containing (sulfonated chitosan:PEO) polymer blend, and all prepared membranes were cross-linked by 2 ml of sulfosuccinic acid as a cross-linker. These free-standing electrolyte samples of approximately 80 μm thickness were subjected to various characterization techniques during the course of the present investigation.

Instrumentation and characterization

FT-IR analysis

The complex formation between the polymer and the nano-composite has been confirmed by Fourier transform infrared spectroscopy (FTIR) spectra using SPECTRA RXI PerkinElmer spectrophotometer in the range of 400–4000 cm^{-1} .

X-ray diffraction

The persuasive evidence for the intercalation of s-SiO₂ could be obtained from XRD patterns of the nano-composites. Radical scan was recorded in the reflection scanning mode with 2θ being changed from 10°–80°. The amorphous nature of the polymer electrolytes has been investigated by X-ray diffraction (XRD) analysis with the help of X'pert PRO PANalytical X-ray diffractometer.

Scanning electron microscopy

The morphology of gold sputter coated composite membranes was examined by scanning electron microscopy (SEM) (FEI Quanta 250 Microscope, Netherlands).

Ionic conductivity

The ionic conductivity of hydrated membranes was measured by impedance spectroscopic technique at different temperatures using a computer controlled μ -autolab type III potentiostat/galvanostat in the frequency range of 10 Hz–1 MHz at room temperature and the signal amplitude of 10 mV which has been designed for through the membrane, to obtain bulk resistance of the membrane. The ionic conductivity values were calculated by using Eq. (1)

$$\sigma = \frac{t}{R_b A} \quad (1)$$

where t and A are the thickness and area of the prepared polymer electrolyte films, respectively. R_b is the bulk resistance of the electrolyte film.

Water uptake

The membranes were immersed in deionized water at room temperature for 48 h. The membranes were then taken out, wiped off the water surface with blotting paper. The wet weight of the membrane was found. Then the membranes were dried under vacuum at 60 °C overnight and weighed. The weight differences before and after the hydration relative to the dry membrane weight were calculated as water uptake percentage using Eq. (2)

$$\text{Water uptake \%} = \frac{W_{\text{wet}} - W_{\text{dry}}}{W_{\text{dry}}} \times 100 \quad (2)$$

Swelling behavior was determined by means of change in surface area and thickness before and after hydration of the membrane. Membrane samples were taken by cutting the membranes in 2 cm \times 2 cm dimensions, and thickness of the membranes was measured with digital micrometer using Eq. (3)

$$\text{Swelling ratio \%} = \frac{T_{\text{wet}} - T_{\text{dry}}}{T_{\text{dry}}} \times 100 \quad (3)$$

Ion exchange capacity

Usual titration method was used to determine the ion exchange capacities (IECs) of the composite membranes. The membranes in their acid form were converted to the

sodium form by immersing 1 M NaCl solution for 24 h at 50 °C in order to exchange H^+ with Na^+ ions, and the solutions were then titrated against 0.1 mol NaOH solutions by using phenolphthalein as the universal indicator. The IEC (meq g^{-1}) values were calculated by using the following Eq. (4)

$$\text{IEC} = (V_{\text{NaOH}})(N_{\text{NaOH}}) / W_{\text{dry}} \quad (4)$$

where V_{NaOH} is the volume of NaOH solution, N_{NaOH} is the normality of NaOH solution, W_{dry} is the mass of the dry sample.

AFM analysis

The tapping mode AFM images of the membranes were acquired in APE Research-Model No: A100SGS. Surface roughness of the membranes was compared using various roughness parameters, such as the mean roughness (R_m), the root mean square of z data (R_q) and the mean difference in the height (R_z). The membrane samples were in dry condition, and the tests were run at the room temperature.

TG analysis

A thermogravimetric analyzer PYRIS Diamond (DSC/TGA SDT Q600) was employed to assess the thermal stability of the HPA-doped nano-composite membranes. The membranes were heated from 20 to 900 °C both at heating rate of 10 °C/min, under a nitrogen atmosphere.

MEA preparation for the PEMFC

The membrane electrode assembly (MEA) was obtained by sandwiching the (s-CS/PEO/PWA(8)/SSA and s-CS/PEO/PMA(6)/SSA) membrane between the anode and the cathode. 40 wt% Pt:C (1:1) on Vulcan XC-72 in both anode and cathode loading (0.5 mg/cm^2) was used as electrocatalyst. This was prepared by incorporating two gas diffusion layers on both sides of membrane. The MEA was assembled in a 5 cm^2 single-cell PEMFC with single serpentine flow fields [Ana bond Sai energy fuel cell technology, Chennai].

Preparation of the anode and cathode

The catalyst slurry inks for the anode and cathode were prepared with the aid of carbon-supported platinum black employing platinum loading $0.025\text{--}0.25 \text{ mg/cm}^2$. Suitable amounts of double distilled water and isopropyl alcohol were mixed with each slurry using an ultra sonicator. After the ultra sonication, the black catalyst slurry was coated onto the respective diffusion layers. The prepared anode and cathode were dried in a vacuum oven at 100 °C for 3 h and then in a box furnace at 380 °C for 7 h.

Result and discussion

FTIR analysis

In Fig. 1, the peaks at 2930 and 2890 cm^{-1} of s-chitosan spectra represent the CH stretching vibrations and 1153 and 1063 peaks represent to saccharide structure (C–O–C vibrations of glucose rings and glycosidic linkage of chitosan [12, 13]. Sulfonated chitosan membrane showed two absorption bands at 1634 and 1567 cm^{-1} which corresponds to characteristic bending vibrations of NH^{3+} group of chitosan membrane. The NH^{3+} group obtained in the membrane results the protonation of NH_2 group by CH_3COOH during dissolution of chitosan [14, 15]. From the FTIR spectra, the peaks at 1650 cm^{-1} for amide I and 1560 cm^{-1} for amide II confirm the presence of amino groups in chitosan molecule [16]. In pure PEO spectrum, a large broad band appears centered at 3446 cm^{-1} . This is due to the hydration of PEO and thus shows that the PEO is highly hydrophilic. Pure PEO shows a large broad band of CH_2 stretching between 2957 and 2840 cm^{-1} [17]. However, in prepared polymer electrolyte the bands are shift to 2918 and 2884 cm^{-1} corresponding to asymmetric CH_2 stretching ($\gamma(\text{CH}_2)_a$) and symmetric CH_2 stretching ($\gamma(\text{CH}_2)_s$) vibrations (Figs. 2, 3), respectively. Two clear vibrational modes appear in PEO at 1464 and 1373 cm^{-1} which corresponds to asymmetric CH_2 bending ($\delta(\text{CH}_2)_a$) and symmetric CH_2 wagging and some C–C stretching ($\omega(\text{CH}_2)_a + \gamma(\text{CC})$) vibrations, respectively.

In Fig. 2 all prepared cross-linked membranes show a peaks at around 3451, 3364 and 3323 cm^{-1} for –OH stretching and NH stretching vibrations, respectively. The bands at 1081, 967, 893, 793 cm^{-1} of the prepared composite membranes are attributed to the stretching vibrations of $\gamma_{\text{as}}(\text{P-O})$, $\gamma_{\text{as}}(\text{M}_0=\text{O})$, $\gamma_{\text{as}}(\text{M}_0-\text{O}_C-\text{M}_0)$ O_C

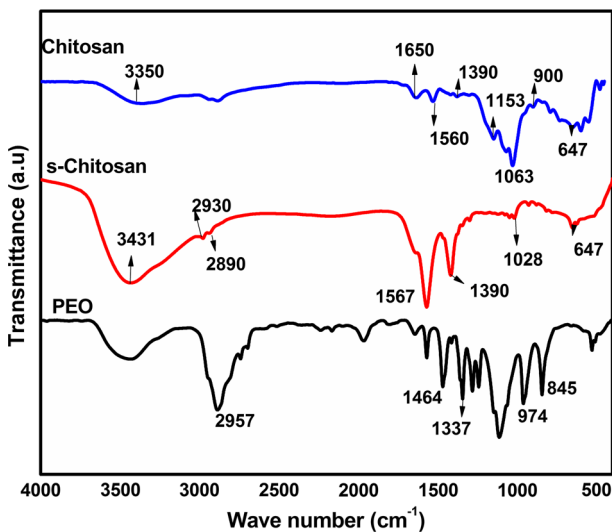


Fig. 1 FTIR spectra of pure PEO, chitosan and s-chitosan

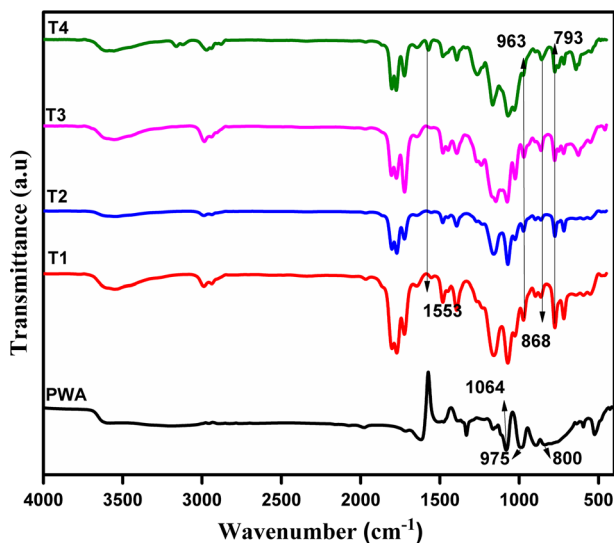


Fig. 2 FTIR spectra of the prepared polymer composite membrane. (T1) s-CS/PEO/PWA(2)/SSA, (T2) s-CS/PEO/PWA(4)/SSA, (T3) s-CS/PEO/PWA(6)/SSA, (T4) s-CS/PEO/PWA(8)/SSA, (T5) s-CS/PEO/PWA(10)/SSA

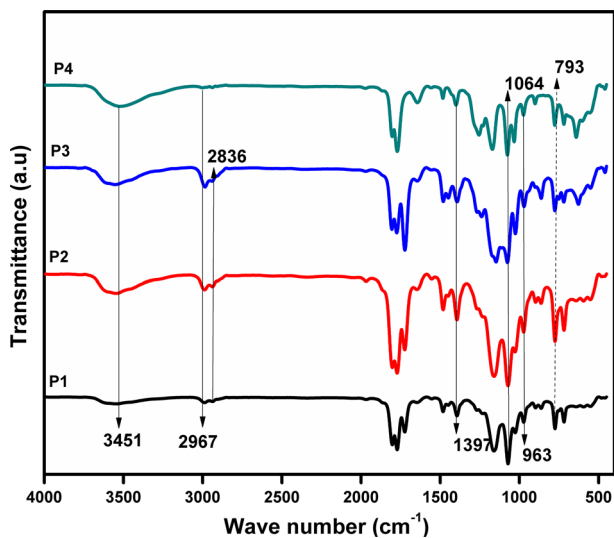


Fig. 3 FTIR spectra of the prepared polymer composite membrane. (P1) s-CS/PEO/PMA(2)/SSA, (P2) s-CS/PEO/PMA(4)/SSA, (P3) s-CS/PEO/PMA(6)/SSA, (P4) s-CS/PEO/PMA(8)/SSA

refers to the center oxygen atom, γ_{as} (M_O-Oe-M_O) refers to the edge oxygen atom which corresponds to PWA- and PMA-doped membrane; these four characteristic peaks are slightly shifted in the complexes, respectively [18].

In all the s-CS/PEO (PWA/PMA)-doped composite membranes showed four characteristic peaks which confirm the Keggin ion geometry in the membrane. In Fig. 2, the peaks at 1550 cm^{-1} attributed to the primary amino groups, which are shifted to 1548 cm^{-1} , respectively. This is due to ionization of the functional group SSA with the amino acid groups of chitosan. From this, the amino group of the chitosan and ionized groups of SSA (sulfonate and two carboxyl groups) could provide the columbic interactions, which results in the electrostatic cross-linking of the chitosan matrix. The sharp peak at 1397 cm^{-1} is evidence peaks of the S=O stretching of the sulfonated groups, respectively. In the higher wave number region of all spectra shows a peak at 1382 cm^{-1} related to $-\text{CH}_3$ symmetric deformation of chitosan [19].

As the HPA content increases, the intensities of their characteristic bands rise. The corner sharing W–O_C–W band (809 cm^{-1}) which corresponds to pure PWA is shifted to higher wave number in PWA-doped membranes. This behavior can be explained by the adequate separation among Keggin units and a vibration less disturbed by anion–anion interactions. The PWA/PMA clusters are probably stabilized in the membranes through a columbic interaction and hydrogen bridges with the inorganic component namely by Si–OH groups [20–23].

XRD analysis

X-ray diffraction patterns for the pure and PWA-/PMA-doped membranes are shown in Figs. 4 and 5. Generally, when a polymer contains a crystalline region, then the X-ray diffraction peaks are sharp and their intensities are high, whereas for

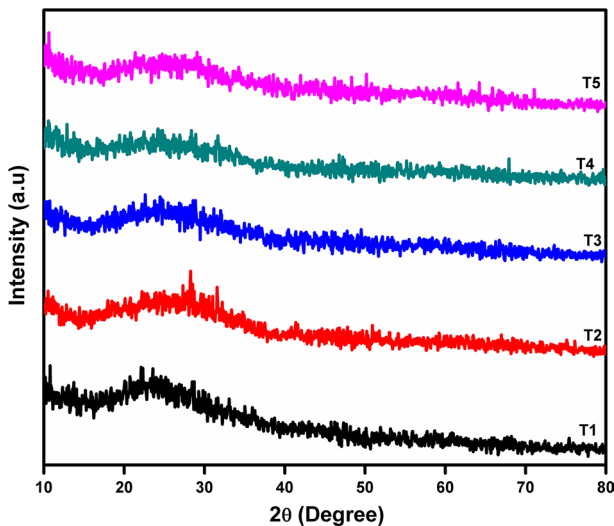


Fig. 4 XRD spectra of the prepared polymer composite membrane. (T1) s-CS/PEO/PWA(2)/SSA, (T2) s-CS/PEO/PWA(4)/SSA, (T3) s-CS/PEO/PWA(6)/SSA, (T4) s-CS/PEO/PWA(8)/SSA, (T5) S-CS/PEO/PWA(10)/SSA

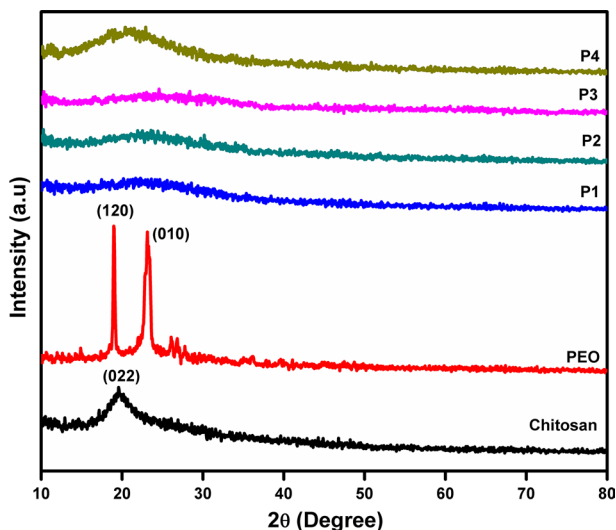


Fig. 5 XRD spectra of pure and the prepared polymer composite membrane. (P1) *s*-CS/PEO/PMA(2)/SSA, (P2) *s*-CS/PEO/PMA(4)/SSA, (P3) *s*-CS/PEO/PMA(6)/SSA, (P4) *s*-CS/PEO/PMA(8)/SSA

an amorphous polymers they are broad [24]. It can be seen that the pure chitosan membrane has the broad peak at 19° (2θ) for the (100) plane (Jcpds. No: 361894) [13]; this indicates an amorphous nature. In Fig. 5, pure PEO peaks are found at $2\theta=19.2^\circ$ and 23.15° corresponds to the reflection of (120) and (010) plane [25], respectively. It confirms the semi-crystalline nature of PEO. The XRD patterns of the HPA-doped membranes have not shown any new diffraction peaks, which implies that the membranes are amorphous. The electrostatic interaction and hydrogen bonding between sulfonated biopolymer and heteropoly acid can contribute to an ordered arrangement of the attached polymer chains.

SEM analysis

Scanning electron microscopy was used to observe the physical structure of the membrane. The electrochemical properties of the membranes are closely related to their micro-structure, especially the spatial distribution of their ionic sites [26]. Figure 6a shows *s*-chitosan/PEO matrix that shows the spherulitic texture is essentially associated with the lamellar structure of the crystalline phase, while the dark regions correspond to partial amorphicity of the biopolymer. From Fig. 6b, the prepared membranes are homogeneous and with obvious no phase separation, which suggests that phosphor tungstic acid does not recrystallize into large particles but interact with *s*-CS/PEO. In Fig. 6c, PMA-doped membrane shows the inorganic phase finely observable defects between the inorganic domain and *s*-chitosan/PEO polymer matrixes. The better dispersion of PWA/SSA in *s*-chitosan/PEO confirms the polar interaction between the acid sites on the surface of HPA and the $-\text{HSO}_3$ groups of

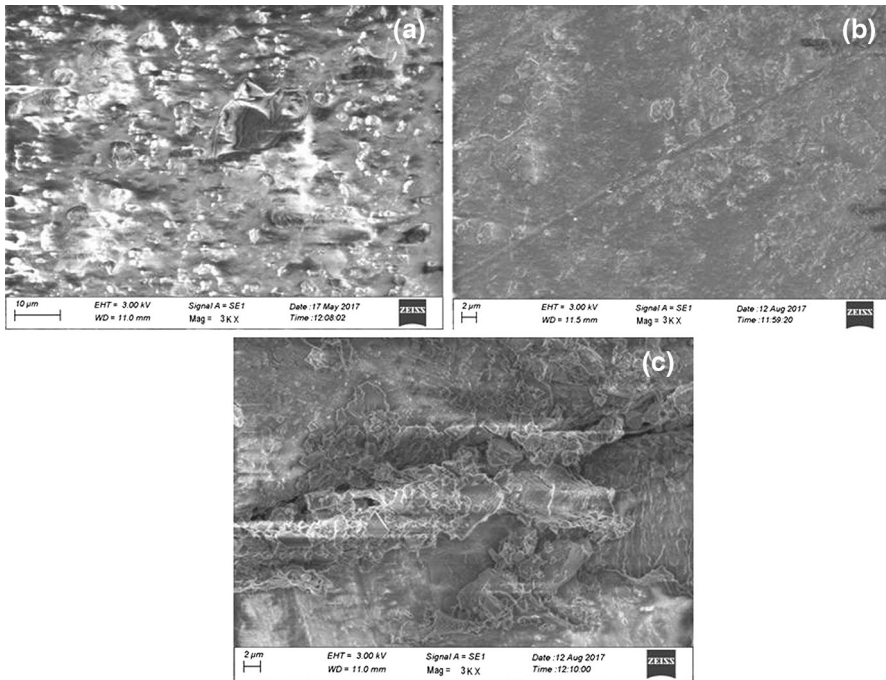


Fig. 6 SEM image of **a** s-CS/PEO, **b** s-CS/PEO/PWA(8)/SSA, **c** s-CS/PEO/PMA(6)/SSA

the polymer matrix which restricted the motion of the SSA in the membrane during the solvent volatilization process.

Conductivity

Ionic conductivity of the prepared polymer electrolyte membrane was determined using the complex impedance method. Typical plots of imaginary impedance (Z'') versus real impedance (Z') for the membranes with varied concentration of PWA/PMA in s-chitosan/PEO (60:40) blend at various temperature. Figures 7 and 8 show the ionic conductivity spectrum of prepared electrolytes. The conductivity values of the prepared membranes are shown in Tables 1 and 2. The increase in the temperature leads to increase in the conductivity because ionic conductivity is in a thermally stimulated process [27]. From Tables 1 and 2, a comparison of both PWA- and PMA-doped membranes higher conductivity is observed with PWA-doped membranes. This is due to the higher number of hydroxyl groups in these membranes with a better capacity to absorb and retain water by hydrogen bonds which is present in the PWA. The amount of water, which occupies the reticular positions in the PWA structure, will enhance the transport of protons through the membrane. Additionally the sulfonation raises the conductivity of the chitosan not only by increasing the number of protonated sites (SO_3H), but also through the formation of water-mediated pathways of protons.

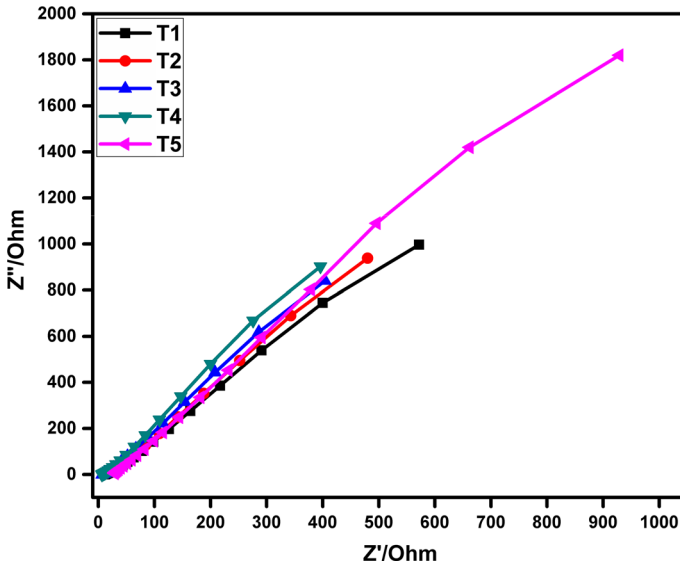


Fig. 7 Conductivity spectrum of prepared electrolytes (T1) s-CS/PEO/PWA(2)/SSA, (T2) s-CS/PEO/PWA(4)/SSA, (T3) s-CS/PEO/PWA(6)/SSA, (T4) s-CS/PEO/PWA(8)/SSA, (T5) s-CS/PEO/PWA(10)/SSA

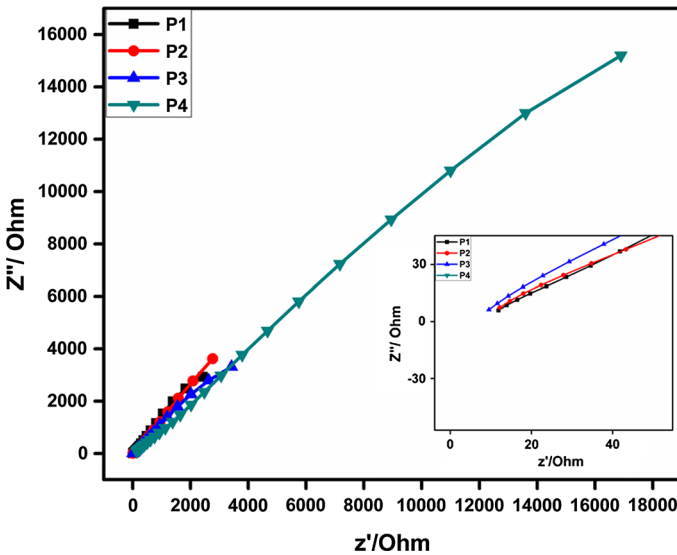


Fig. 8 Conductivity spectrum of prepared electrolytes (P1) s-CS/PEO/PMA(2)/SSA, (P2) s-CS/PEO/PMA(4)/SSA, (P3) s-CS/PEO/PMA(6)/SSA, (P4) s-CS/PEO/PMA(8)/SSA

Table 1 Conductivity values for the prepared polymer electrolyte with different ratios of PWA as a dopant in s-CS/PEO cross-linked membranes

Sample code	Ratio (s-CS:PEO)/ PWA/SSA (2 ml)	Conductivity $\sigma / \times 10^{-2} \text{ S cm}^{-1}$					
		303 K	313 K	323 K	333 K	343 K	353 K
T1	98:02	1.37	1.44	1.610	1.763	2.012	2.295
T2	96:04	2.51	2.45	2.74	2.79	2.95	3.21
T3	94:06	3.41	3.67	3.81	3.99	4.21	4.57
T4	92:08	4.85	5.46	7.92	8.10	8.99	9.21
T5	90:10	3.26	3.79	4.19	5.84	6.19	6.54

Table 2 Conductivity values for the prepared polymer electrolyte with different ratios of PMA as a dopant in SCS/PEO cross-linked membranes

Sample code	Ratio (s-CS:PEO)/ PWA/SSA (2 ml)	Conductivity $\sigma / \times 10^{-3} \text{ S cm}^{-1}$					
		303 K	313 K	323 K	333 K	343 K	353 K
P1	98:02	1.21	2.045	2.100	2.35	2.56	2.85
P2	96:04	2.02	2.81	3.03	3.23	4.97	5.20
P3	94:06	3.543	4.06	4.440	5.866	6.010	6.752
P4	92:08	3.180	3.381	3.89	4.573	4.888	5.01

Temperature dependency of conductivity

The membrane exhibits an increase in ionic conductivity with increasing temperature and reaches the highest conductivity in the tested temperature. As proton conductivity is thermally stimulated, it is reasonable to expect a rise in conductivity with temperature and higher dehydration of the membrane with higher temperature. Thus, it is very important the capacity to retain water at higher temperature. The change of conductivity with temperature follows the Arrhenius relations as shown in Figs. 9 and 10.

In solid PWA with crystalline water, the ion migration can be ascribed to the vehicle mechanism. But in the prepared membrane exhibit both vehicle and Grotthuss mechanism for the proton transportation because the value of activation energy of the membrane falls below the value 1 eV as already reported by the Smitha et al. [28]. Figs. 9 and 10 provide a comparison among the activation energies of PWA-doped membranes and PMA-doped membranes, calculated from the Arrhenius equation. With increasing PWA, more routes for protons transportation are created and consequently, the activation energy is decreased. In other words, with increasing PWA groups the ionic domains become more interconnected and result in more facilitated proton diffusion. The activation energy of proton transfer through PWA filled membranes was lower than that for corresponding PMA filled membranes. Such an observation could be interpreted in terms of the ability of PWA molecules

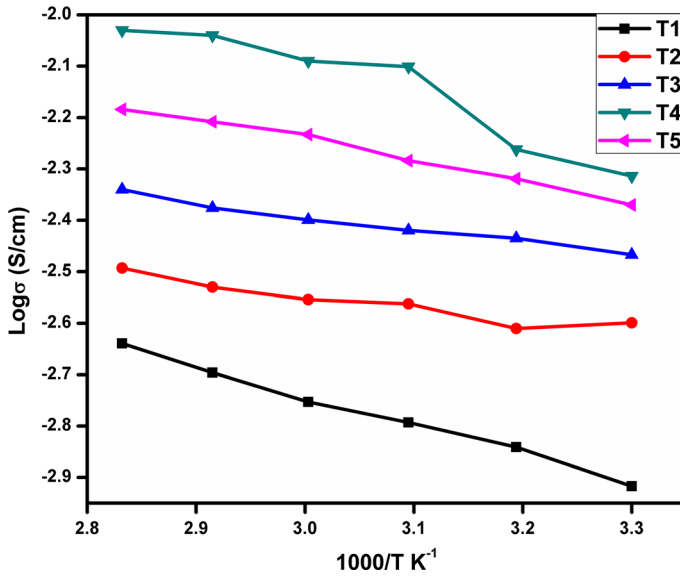


Fig. 9 Temperature dependence conductivity spectra of prepared electrolytes of (T1) *s*-CS/PEO/PWA(2)/SSA, (T2) *s*-CS/PEO/PWA(4)/SSA, (T3) *s*-CS/PEO/PWA(6)/SSA, (T4) *s*-CS/PEO/PWA(8)/SSA, (T5) *s*-CS/PEO/PWA(10)/SSA

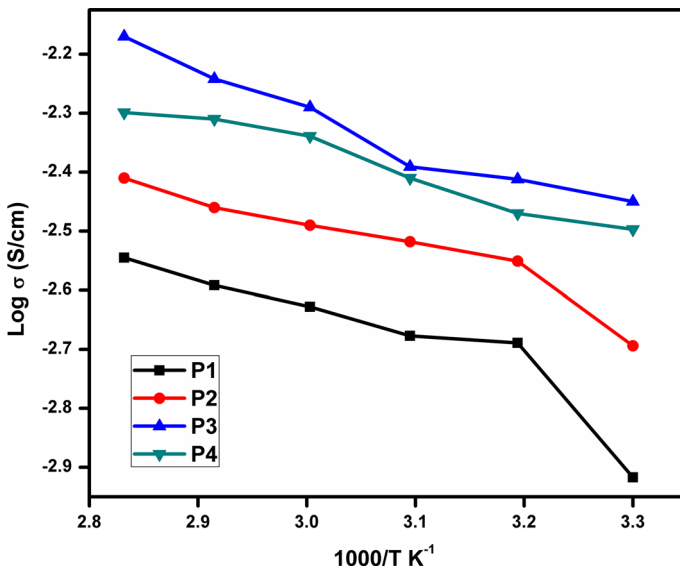


Fig. 10 Temperature dependence conductivity spectra of prepared electrolytes of (P1) *s*-CS/PEO/PMA(2)/SSA, (P2) *s*-CS/PEO/PMA(4)/SSA, (P3) *s*-CS/PEO/PMA(6)/SSA, (P4) *s*-CS/PEO/PMA(8)/SSA

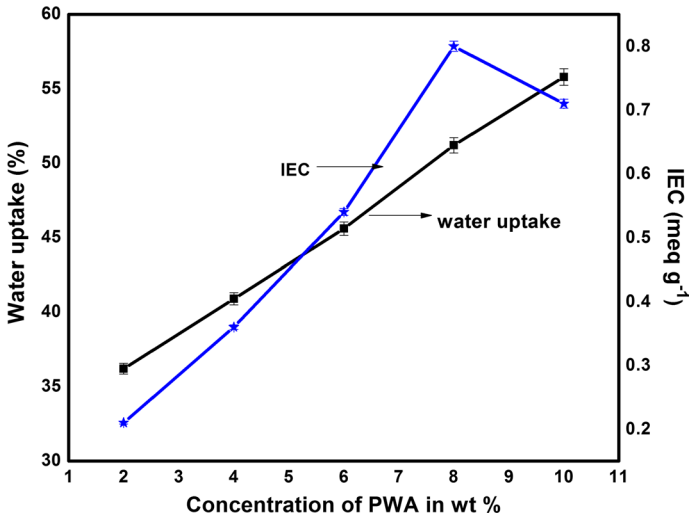


Fig. 11 Water uptake and IEC spectra of s-chitosan/PEO with different weight ratio of PWA(2, 4, 6, 8, 10)/SSA

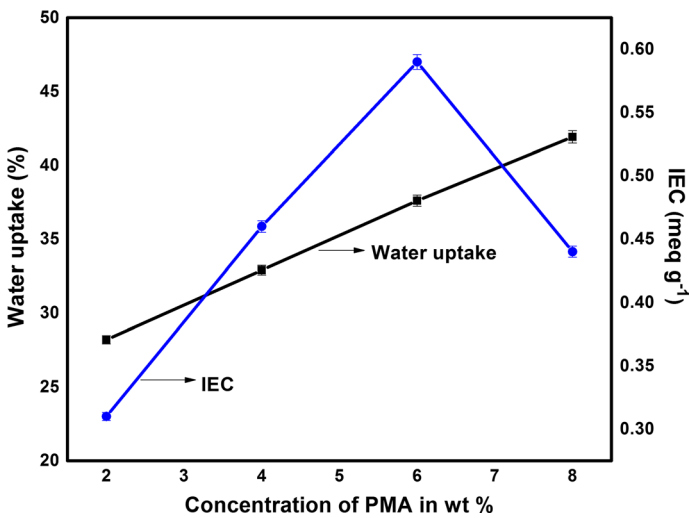


Fig. 12 Water uptake and IEC spectra of s-chitosan/PEO with different weight ratio of PMA(2, 4, 6, 8)/SSA

to raise the water content in the polyelectrolyte matrices by providing extra water sorption sites, which results in the proton conduction being expedited.

Table 3 Values of physicochemical studies as a function of PWA with different ratios in sulfonated chitosan/PEO blended membrane

Sample code	Ratio (s-CS:PEO)/ PWA/SSA	Water uptake/%	Swelling ratio/%	IEC/meq g ⁻¹
T1	98:02	36.2	23	0.21
T2	96:04	40.9	25.2	0.36
T3	94:06	45.6	29.5	0.54
T4	92:08	51.2	20.9	0.80
T5	90:10	55.8	19	0.71

Table 4 Values of physicochemical studies as a function of PMA with different ratios in sulfonated chitosan/PEO blended membrane

Sample code	Ratio (s-CS:PEO)/ PMA/SSA	Water uptake/%	Swelling ratio/%	IEC/meq g ⁻¹
P1	98:02	28.2	18	0.31
P2	96:04	32.9	21	0.46
P3	94:06	37.6	19.5	0.59
P4	92:08	41.92	20.9	0.44

Physico-chemical characterizations

Water uptake and swelling ratio

The swelling property has a profound effect on proton transport and dimensional stability of proton conducting membrane. Proton transport requires a significant amount of water to coordinate with protons. Excessively high water uptake can change the membrane dimensional. Figures 11 and 12 show the room-temperature water uptake as a function of different weight ratios of PWA-/PMA-doped composite membranes. The sulfonated biopolymer/PEO/PWA water uptake is greater than that of PMA-doped membrane. Water content of the PWA membrane increases owing to the incorporation of hydrophilic groups upon sulfonation. Thus, incorporation of polar groups on sulfonating the polymer and reduction in the number of polar groups in the doped polymer together result in reasonable and sufficient water sorption.

Ion exchange capacity

IEC indicates the amount of the ion exchangeable group present in a polymer matrix which is responsible for proton transfer and thus is an indirect and reliable approximation of the ion conductivity [29]. Increase in water uptake confirms to the change tendency of ion exchange capacity indicating the strong dependency of membranes

hydrophilicity on their IEC value. From Tables 3 and 4, the value of IEC of PWA-doped membrane is higher than the PMA-doped membrane.

This was attributed to the interacted functional groups of $-\text{COOH}$ and sulfonic groups with PWA. These reacted functional groups in the membrane would contribute in increasing the ionic conductivity which indicates that a large PWA/SSA content plays a major role in controlling the ion conduction due to unity, which suggests increased sulfonic acid groups in the membrane. When the membrane is cross-linked by SSA, the IEC values increase due to the rich SO_3H^+ ions.

Surface roughness analysis of the membranes

The difference in the morphology can be expressed in terms of various roughness parameters such as the mean roughness (R_a), the root mean square (rms) of vertical data (R_q) and the maximum height R_{max} . Here the mean roughness is the mean value of surface relative to the center plane; the plane for which the volume enclosed by the image above and below this plane is equal. R_{max} is the height difference between the highest and lowest points on the surface relative to the membrane plane, and R_q is the standard deviation of the z values within the given area [30]. The topographic image of s-CS/PEO exhibits smooth and homogeneous surface morphology which is shown in Fig. 13a. In contrast, the surface morphology of s-CS/PEO/HPA-doped membrane is considerably rougher than pure CS/PEO membrane. Figure 13b, c shows an AFM 3D image of the top surface morphology for the s-CS/PEO/PWA and s-CS/PEO/PMA bio-composite membrane, which shows some nodule size and roughness. The relatively lighter parts correspond to the softer hydrophilic ionic cluster domains of the s-chitosan/PEO matrix. The mean roughness for the surface topography of the membrane (R_a) was 29.3 and 18.4 nm. It was clearly indicated

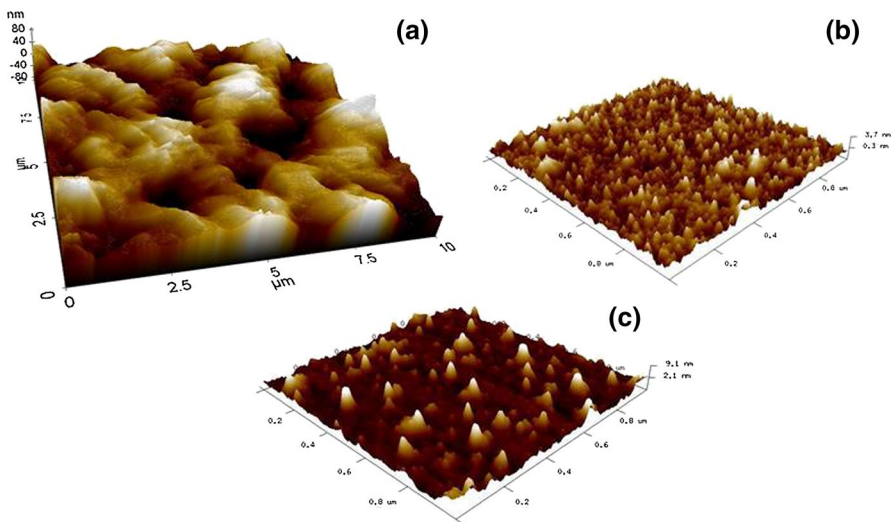
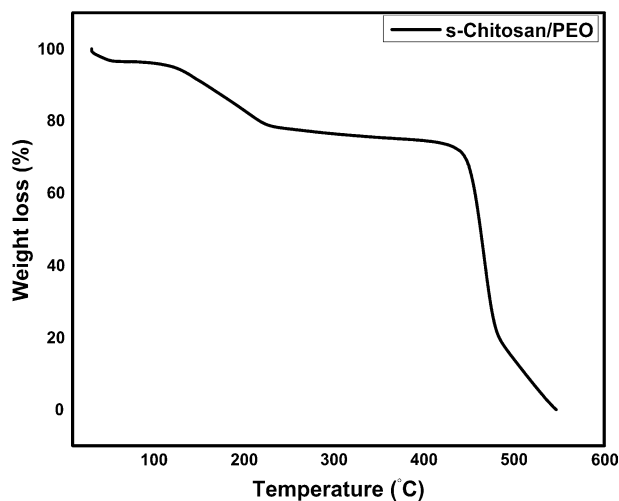
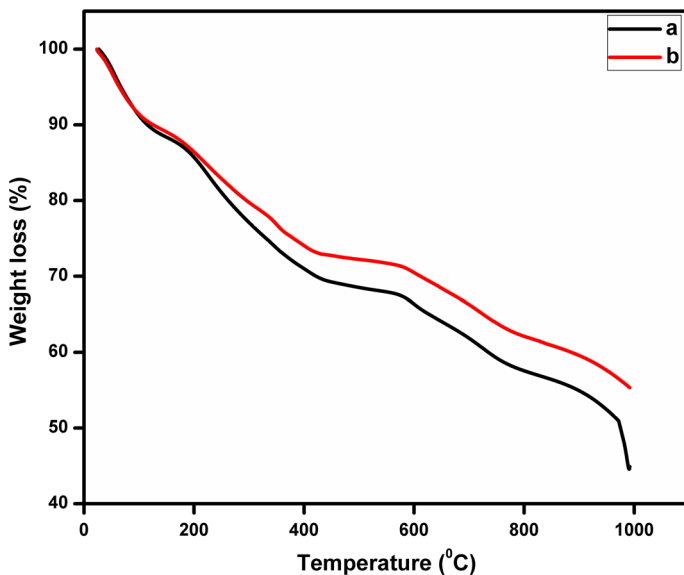


Fig. 13 AFM image of a s-CS/PEO, b s-CS/PEO/PWA(8)/SSA, c s-CS/PEO/PMA(6)/SSA

Table 5 Roughness parameters of the PWA-/PMA-doped prepared electrolyte membranes

Sample	Roughness parameters		
	R_m (nm)	R_q (nm)	R_z (nm)
s-CS/PEO/PWA(8 wt%)/SSA	29.3	9.42	7.55
s-CS/PEO/PMA(6 wt%)/SSA	18.4	2.12	1.56

**Fig. 14** TG analysis spectra of s-chitosan/PEO prepared electrolyte membranes**Fig. 15** TG analysis spectra of prepared electrolyte membranes (a) s-CS/PEO/PMA(6 wt%)/SSA, (b) s-CS/PEO/PWA(8 wt%)/SSA

that the compatibility of the s-CS/PEO composite membrane is good. A lot of small hump with RMS value of 9.42 nm (Table 5) is observed in the PWA-doped prepared composite membrane.

Thermal stability

Thermal analysis (TG) was employed to investigate the thermal stability of the prepared polymer composite membranes. Figures 14 and 15 show the weight loss curves of the s-chitosan/PEO and cross-linked s-chitosan/PEO/(PWA/PMA)-doped membranes. There are three major weight loss stages around 120–200, 380–510 and 710 °C in the tested temperature range. In the first stage, the weight loss is due to the degradation of small molecules, physically absorbed water and residual solvent. The second weight loss is attributed to the release of structural water from PWA, and the third weight loss is referred to structure collapse of PWA and thermal decomposition of polymer network [31]. In PMA-doped membrane, each weight loss step is responsible for a thermal salvation, thermal degradation of the cross-links and finally a thermal oxidation of the polymer chain, respectively. The weight loss of the membrane is due to the thermal degradation of the cross-linkages of the membrane, and the third weight loss is due to degradation of the polymer back bone.

Membrane stability

Addition to high proton conductivity, membranes used for fuel cell applications must also possess acceptable hydrolytic stability to retain conductivity at operational conditions. The hydrolytic stability of the fabricated membranes was evaluated through comparison of proton conductivity and IEC before and after soaking the membranes in 30 °C water for 2 weeks. As discussed earlier, increase in PWA, on the one hand, improves proton conductivity but, on the other hand, results in the hydrolytic stability of s-CS/PEO matrices to be decreased. It was found that s-CS/PEO membranes with PMA exhibited sufficient hydrolytic stability. The obtained results revealed that the conductivity of membranes with 2, 4, 6, 8 and 10 wt%, after soaking in 30 °C water for 2 weeks, was decreased from 1.37, 2.51, 3.43, 4.85 and 3.26×10^{-2} S/cm to 0.87, 1.17, 1.89, 2.68, and 2.5×10^{-2} S/cm, respectively. Such negligible changes in proton conductivity could be ascribed to the partial decomposition of the sulfonic acid groups in an aqueous environment. It is expected that an acceptable hydrolytic stability of prepared polymer electrolytes could be ensured owing to the large molecular size of PWA.

PEMFC performances of the membrane

Considering the unique advantages of the low-temperature PEM fuel cell and the superior conductivity of the HPA-doped hybrid membranes, the single-cell performance was measured under room temperature. Due to the good comprehensive performances of proton conductivity and structural stability s-CS/PEO/PWA(8)/SSA and s-CS/PEO/PMA(6)/SSA membranes were chosen as representatives and then

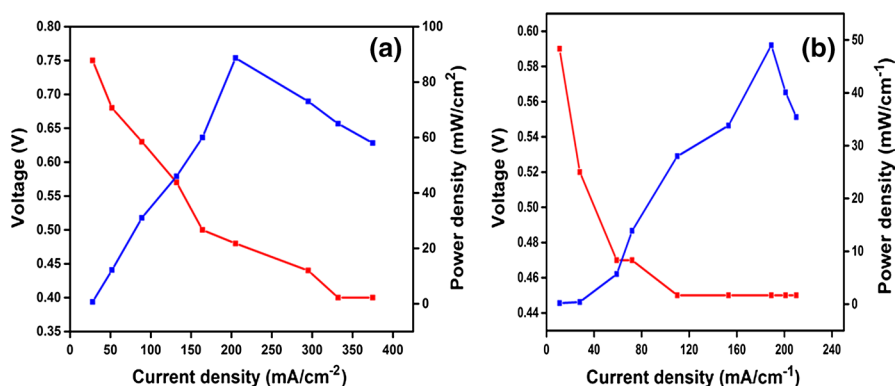


Fig. 16 Polarization curve of (a) s-CS/PEO/PWA(8)/SSA (b) s-CS/PEO/PMA(6)/SSA prepared electrolytes

measured under 30 °C (0% RH) uniform thickness which was utilized for each membrane to ensure a good comparison. Figure 16 shows that s-CS/PEO/PWA(8)/SSA membrane attains the voltage 0.75 V inferring a good H₂ barrier ability. The current density for s-CS/PEO/PWA(8)/SSA and s-CS/PEO/PMA(6)/SSA was measured to be 375 and 210 mA/cm² (0.02 V potential at 30 °C). The maximum power density for these membranes at the maximum point was also obtained as 88.7 and 49 mW/cm², respectively. The observed results could be attributed to the tight structure of cross-linked sulfonated chitosan/PEO membrane at low temperature. According to the obtained results, prepared membranes could have promising potential in low-temperature PEM fuel single cell under real conditions.

Conclusions

Hybrid polymer electrolyte membranes were developed by doping the heteropoly acids in sulfonated bio polymer bended with PEO matrix. FTIR spectroscopy was used to characterize the chemical cross-linking reaction of the doped HPA membranes. Cross-linking helps to increase the conductivity and thermal stability of the heteropoly acid-doped membranes. The obtained ionic conductivity of the PWA-doped membranes is in the order of 10⁻² S/cm and the PMA-doped membranes are in the 10⁻³ S/cm. From results the PWA-doped sulfonated chitosan/PEO matrix has equal conductivity of the commercially available membrane Nafion 117 which has fluorine chemical structure. The topographical feature of the membrane surface was successfully characterized by atomic force microscopy in tapping mode. The composite membrane which contains s-CS/PEO/PWA (8 wt%) with 2 ml of SSA cross-linked membrane had high conductivity, lower swelling ratio, highest IEC and enhanced thermal stability among all the other doped membranes. Synthesized membranes showed several favorable properties including convenient preparation and low cost. Considering these advantages besides the obtained results of

single-cell low-temperature PEMFC performance tests, such bio-resource proton conducting materials could be hopeful in the field of fuel cell applications.

Compliance with ethical standards

Conflict of interest The authors declare that they have no conflict of interest.

References

1. Santamaria M, Pecorara CM, Franco FD, Quarto FD (2017) Phosphomolybdic acid and mixed phosphotungstic/phosphomolybdic acid chitosan membranes as polymer electrolytes for H₂/O₂ fuel cells. *Int J Hydrog Energy*. <https://doi.org/10.1016/j.ijhydene.2017.02.069>
2. Lin CW, Thangamuthu R, Chang PH (2005) PWA-doped PEG/SiO₂ proton-conducting hybrid membranes for fuel cell applications. *J Membr Sci* 254:197–205. <https://doi.org/10.1016/j.memsci.2005.01.007>
3. Honma I, Nomura S, Nakajima H (2001) Proton conducting organic/inorganic nano composites for polymer electrolyte membrane. *J Membr Sci* 185:83–94. [https://doi.org/10.1016/s0376-7388\(00\)00636-0](https://doi.org/10.1016/s0376-7388(00)00636-0)
4. Yang J, Janik MJ, Ma D, Zheng A, Zhang M, Neurock M, Davis RJ, Ye C, Deng F (2005) Location, acid strength, and mobility of the acidic protons in Keggin 12–H₃PW₁₂O₄₀: a combined solid-state NMR spectroscopy and DFT quantum chemical calculation study. *J Am Chem Soc* 127:18274–18280. <https://doi.org/10.1021/ja055925z>
5. Tang HL, Pan M, Lu SF, Lu JL, Jiang SP (2010) One-step synthesized HPW/meso-silica inorganic proton exchange membranes for fuel cells. *Chem Commun* 46:4351–4353. <https://doi.org/10.1039/c003129a>
6. Ma J, Sahai Y (2013) Chitosan biopolymer for fuel cell applications. *Carbohydr Polym* 92:955–975. <https://doi.org/10.1016/j.carbpol.2012.10.015>
7. Rinaudo M (2006) Chitin and chitosan: properties and applications. *Prog Polym Sci* 31:603–663. <https://doi.org/10.1016/j.progpolymsci.2006.06.001>
8. Hejazi R, Amiji M (2003) Chitosan-based gastrointestinal delivery systems. *J Control Release* 89:151–165. [https://doi.org/10.1016/s0168-3659\(03\)00126-3](https://doi.org/10.1016/s0168-3659(03)00126-3)
9. Gil ES, Hudson SM (2004) Stimuli-responsive polymers and their bioconjugates. *Prog Polym Sci* 29:1173–1222. <https://doi.org/10.1016/j.progpolymsci.2004.08.003>
10. Kim H, Kang MS, Lee DH, Won J, Kim J, Kang YS (2007) Proton exchange membranes with high cell performance based on Nafion/poly (*p*-phenylene vinylene) composite polymer electrolyte. *J Membr Sci* 304:60–64. <https://doi.org/10.1016/j.memsci.2007.06.049>
11. Tsai HS, Wang YZ, Lin JJ, Lien WF (2010) Preparation and properties of sulfo propyl chitosan derivatives with various sulfonation degree. *J Appl Polym Sci* 116:1686–1693. <https://doi.org/10.1002/app.31689>
12. Bostan MS, Muthu EC, Kazak H, Keskin SS, Oner ET, Eroglu MS (2014) Comprehensive characterization of chitosan/PEO/levan ternary blend films. *Carbohydr Polym* 102:993. <https://doi.org/10.1016/j.carbpol.2013.09.096>
13. Dorraki N, Safa NN, Jahanfar M, Ghomi H, Siadat SOR (2015) Surface modification of chitosan/PEO nanofibers by air dielectric barrier discharge plasma for acetylcholinesterase immobilization. *Appl Surf Sci* 349:940–947. <https://doi.org/10.1016/j.apsusc.2015.03.118>
14. Cui Z, Xiang Y, Si J, Yang M, Zhang Q, Zhang T (2008) Ionic interactions between sulfuric acid and chitosan membranes. *Carbohydr Polym* 73:111–116. <https://doi.org/10.1016/j.carbpol.2007.11.009>
15. Cui Z, Liu C, Lu T, Xing W (2007) Polyelectrolyte complexes of chitosan and phosphotungstic acid as proton-conducting membranes for direct methanol fuel cells. *J Power Sources* 167:94–99. <https://doi.org/10.1016/j.jpowsour.2006.12.112>
16. Yuan W, Wu H, Zheng B, Zheng X, Jiang Z, Hao X, Wang B (2007) Sorbitol-plasticized chitosan/zeolite hybrid membrane for direct methanol fuel cell. *J Power Sources* 172:604–612. <https://doi.org/10.1016/j.jpowsour.2007.05.040>

17. Fournier M, Thouvenot R (1983) Vibrational investigations of polyoxometalates. 2. Evidence for anion–anion interactions in molybdenum(VI) and tungsten(VI) compounds related to the Keggin structure. *Inorg Chem* 22:207–216
18. Choudhury NA, Ma J, Sahai Y (2012) High performance and eco friendly chitosan hydrogel membrane electrolytes for direct borohydride fuel cells. *J Power Sources* 210:358–365. <https://doi.org/10.1016/j.jpowsour.2012.03.013>
19. Selvasekarapandian S, Baskaran R, Hema M (2005) Complex AC impedance, transference number and vibrational spectroscopy studies of proton conducting PVAc–NH₄SCN polymer electrolytes. *Phys B* 357:412–419. <https://doi.org/10.1016/j.physb.2004.12.007>
20. Staiti P, Freni S, Hocevar S (1999) Synthesis and characterization of proton-conducting materials containing dodecatungstophosphoric and dodecatungstosilic acid supported on silica. *J Power Sources* 79:250–255. [https://doi.org/10.1016/s0378-7753\(99\)00177-9](https://doi.org/10.1016/s0378-7753(99)00177-9)
21. Yin Y (2015) Hybrid/composite membranes. In: Fang J, Qiao J, Wilkinson DP, Zhang J (eds) *Electrochemical polymer electrolyte membranes*. CRC Press, Boca Raton, pp 365–448. <https://doi.org/10.1201/b18369-10>
22. Kim H, Lee YM (2001) Gas permeation properties of poly(amide-6-b-ethylene oxide)–silica hybrid membranes. *J Membr Sci* 193:209–225. [https://doi.org/10.1016/s0376-7388\(01\)00514-2](https://doi.org/10.1016/s0376-7388(01)00514-2)
23. Zhao Y, Jiang Z, Xiao L, Xu T, Qiao S, Wu H (2011) Chitosan membranes filled with biomimetic mineralized hydroxyapatite for enhanced proton conductivity. *Solid State Ionics* 187:33–38. <https://doi.org/10.1016/j.ssi.2011.01.019>
24. Tseng CY, Ye YS, Kao KY, Joseph J, Shen WC, Rick J, Hwang BJ (2011) Interpenetrating network-forming sulfonated poly (vinyl alcohol) proton exchange membranes for direct methanol fuel cell applications. *J Hydrog Energy* 36:11936–11945. <https://doi.org/10.1016/j.ijhydene.2011.06.025>
25. Ye YS, Yen YC, Cheng CC, Cheng WY, Tsai LT, Chang FC (2009) Sulfonated poly(ether ether ketone) membranes crosslinked with sulfonic acid containing benzoazine monomer as proton exchange membranes. *Polymer* 50:3196–3203. <https://doi.org/10.1016/j.polymer.2009.04.072>
26. Anis A, Banthia AK, Bandyopadhyay S (2008) Synthesis and characterization of PVA copolymer/phosphomolybdic acid based crosslinked composite polymer electrolyte membrane. *J Power Sources* 179:69–80. <https://doi.org/10.1016/j.jpowsour.2007.12.041>
27. Aparicio M, Mosa J, Etienne M, Duran A (2005) Proton conducting methacrylate silica sol–gel membranes containing tungstophosphoric acid. *J Power Sources* 145:231–236. <https://doi.org/10.1016/j.jpowsour.2005.01.071>
28. Smitha B, Sridhar S, Khan AA (2004) Polyelectrolyte complexes of chitosan and poly(acrylic acid) as proton exchange membranes for fuel cells. *Macromolecules* 37:2233–2239. <https://doi.org/10.1021/ma0355913>
29. Wu YH, Wu CM, Yu F, Xu TW, Fu YX (2008) Free standing anion-exchange PEO–SiO₂ hybrid membranes. *J Membr Sci* 307:28–36. <https://doi.org/10.1016/j.memsci.2007.07.043>
30. Stangar UL, Grosej N, Orel B, Colombar P (2000) Structure of and interactions between P/SiWA Keggin nanocrystals dispersed in an organically modified electrolyte membrane. *Chem Mater* 12:3745–3753. <https://doi.org/10.1021/cm0010046>
31. Aparicio M, Castro Y, Duran A (2005) Synthesis and characterisation of proton conducting styrene-co-methacrylate–silica sol–gel membranes containing tungstophosphoric acid. *Solid State Ionics* 176:333–340. <https://doi.org/10.1016/j.ssi.2004.07.021>